Dual-network bacterial cellulose-based separators with high wet strength and dual ion transport mechanism for uniform lithium deposition

Chen Cheng[a], Rendang Yang[a], Yang Wang[a,b]*, Xiaohui Guo[a], Jie Sheng[c]

[a] *State Key Laboratory of Pulp and Paper Engineering, South China University of Technology, Guangzhou 510640, China*

[b] *School of Chemistry and Chemical Engineering, South China University of Technology, Guangzhou 510640, China*

[c] *School of Environmental and Chemical Engineering, Foshan University, Foshan 528000, China*

Corresponding Author: E-mail: misteryang@163.com.

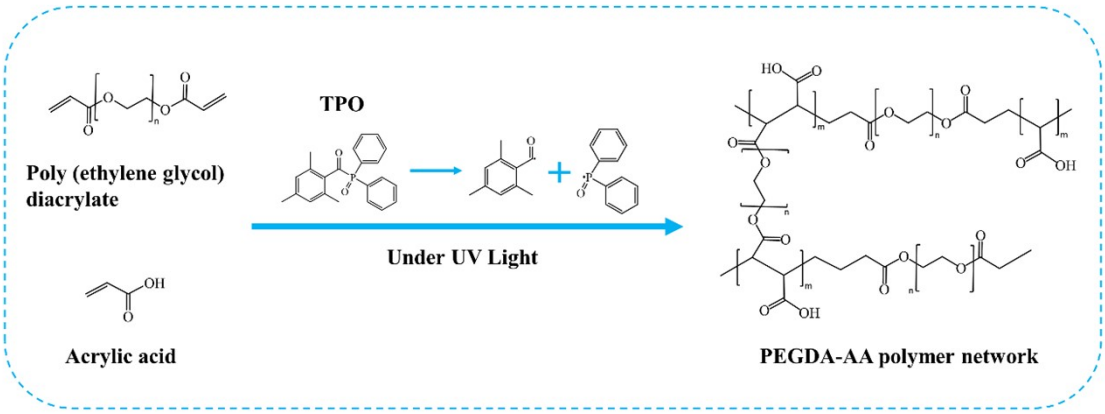

Figure S1. UV-Photopolymerization mechanism of polymer network.

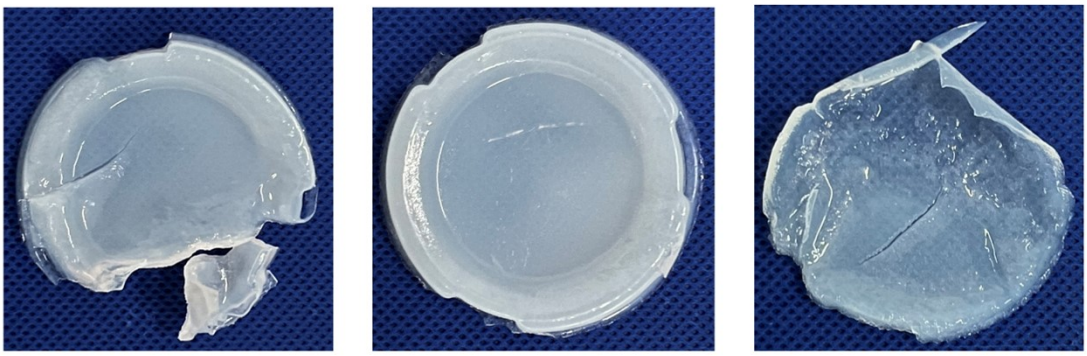

Figure S2. Morphology of polymer gel after polymerization with different concentrations of photoinitiator.

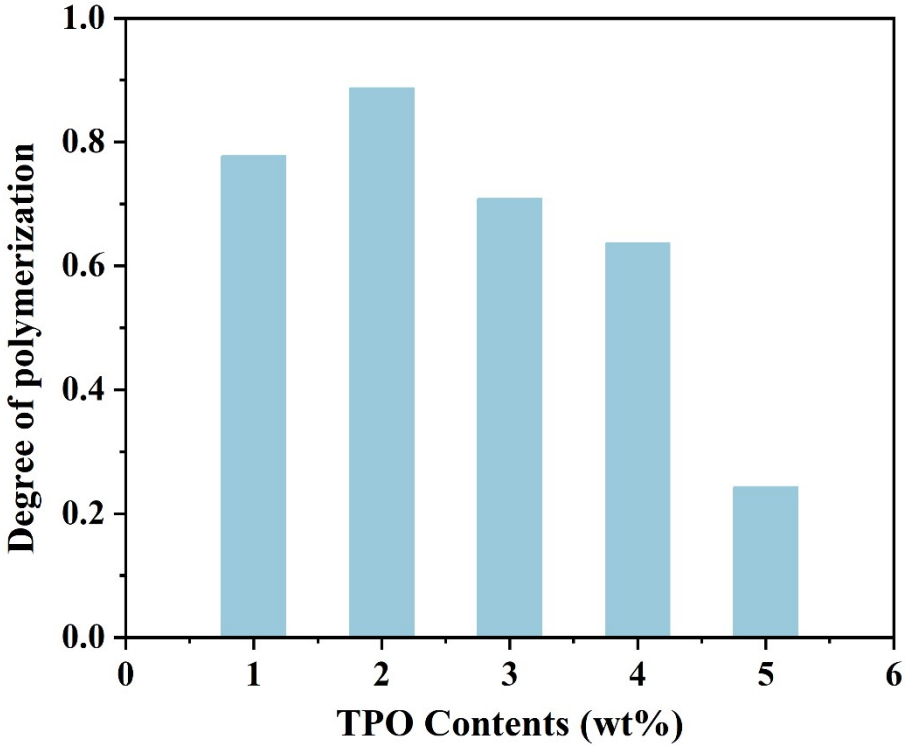

Figure S3. Degree of polymerization of polymer gel after polymerization with different concentrations of photoinitiator.

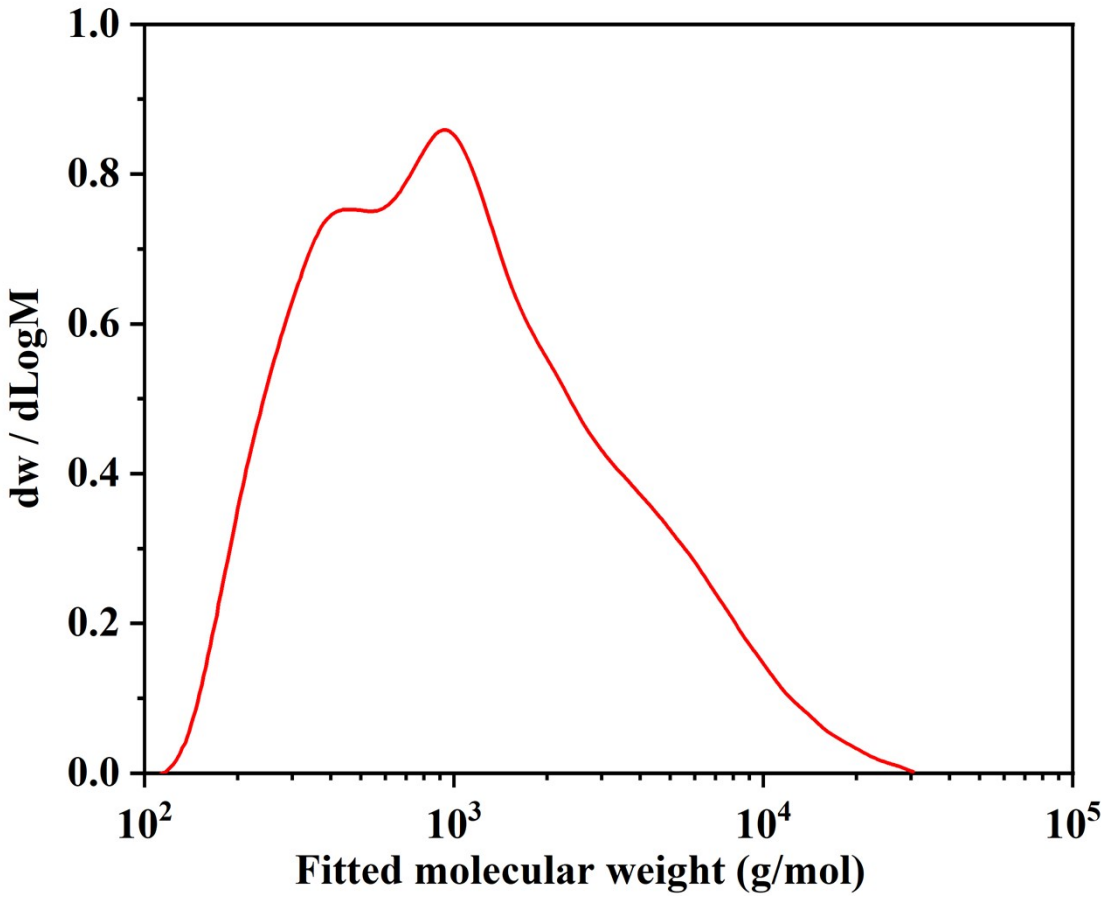

Figure S4. Molecular weight distribution of PEGDA and AA copolymer.

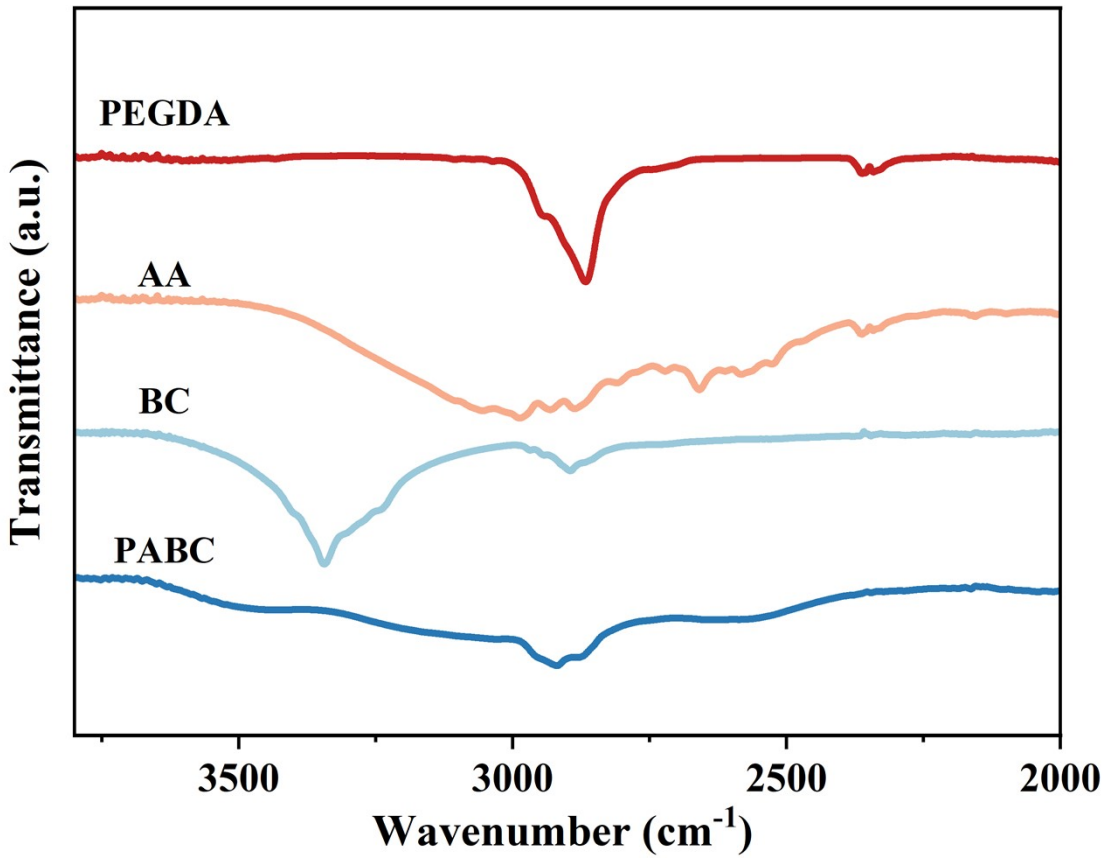

Figure S5. ATR spectrum of different separators.

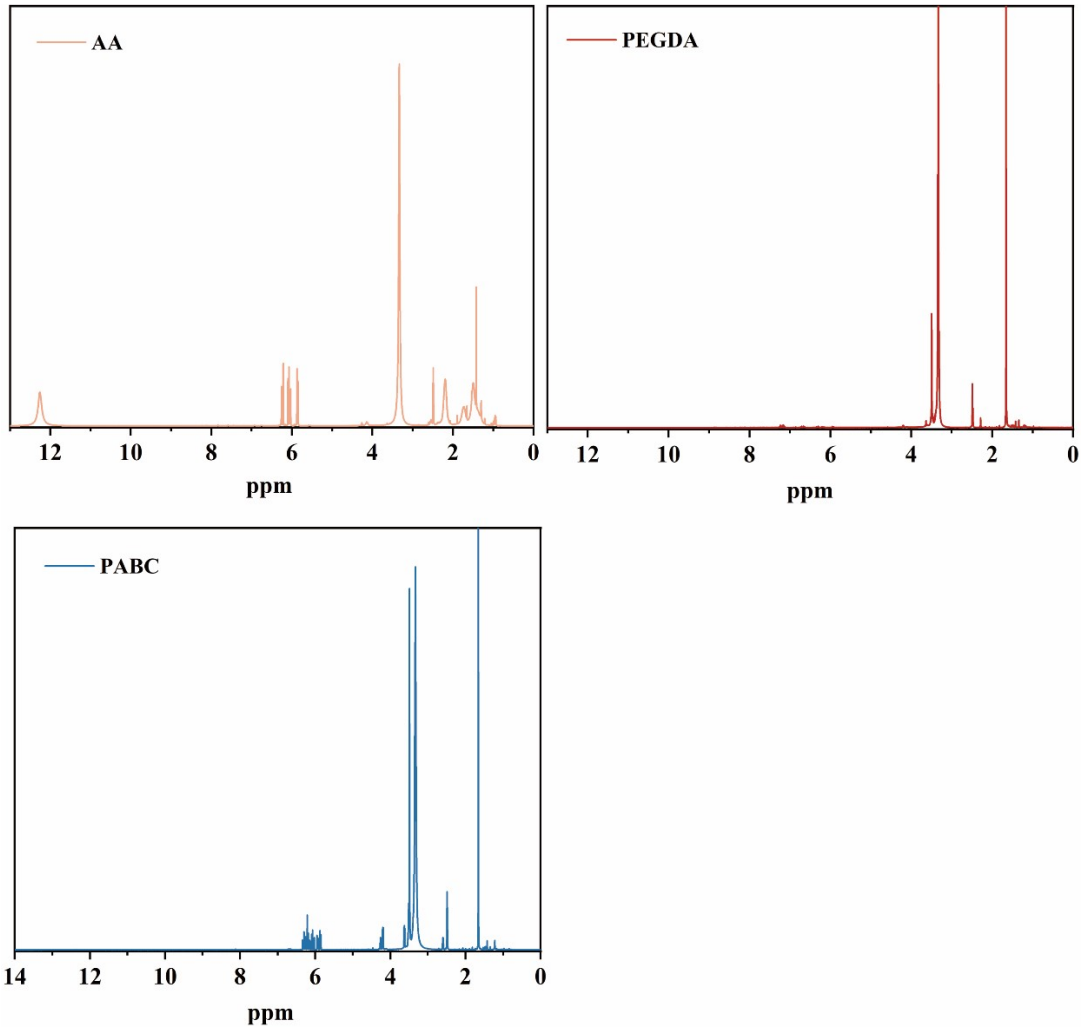

Figure S6. ^{1}H-NMR spectra of AA, PEGDA and PABC after polymerization.

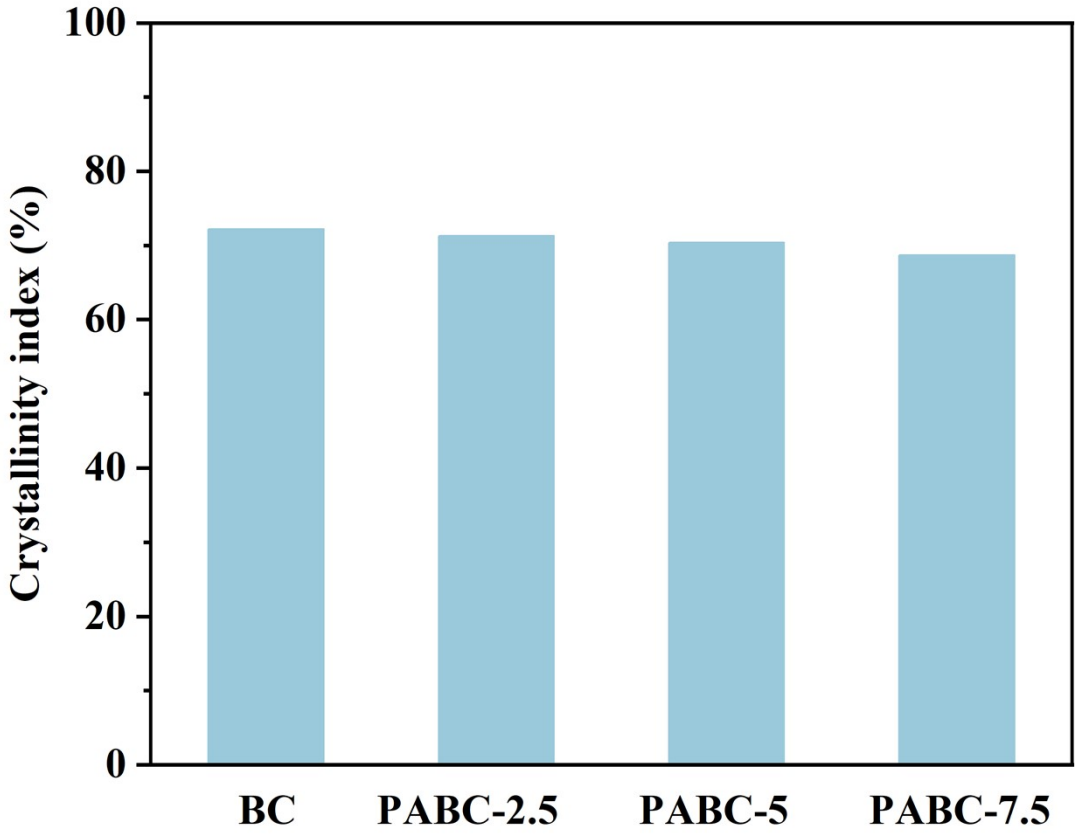

Figure S7. Comparison of crystallinity of different separators.

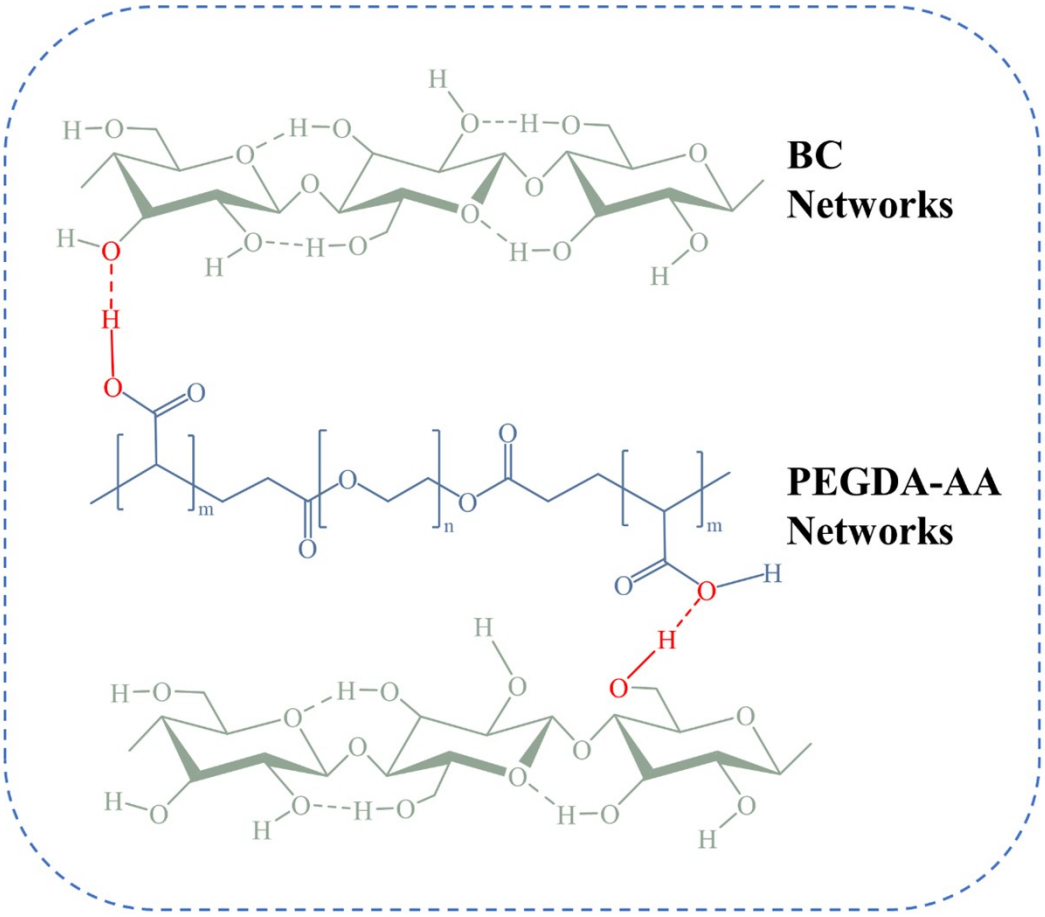

Figure S8. Interactions between BC and PEGDA-AA networks.

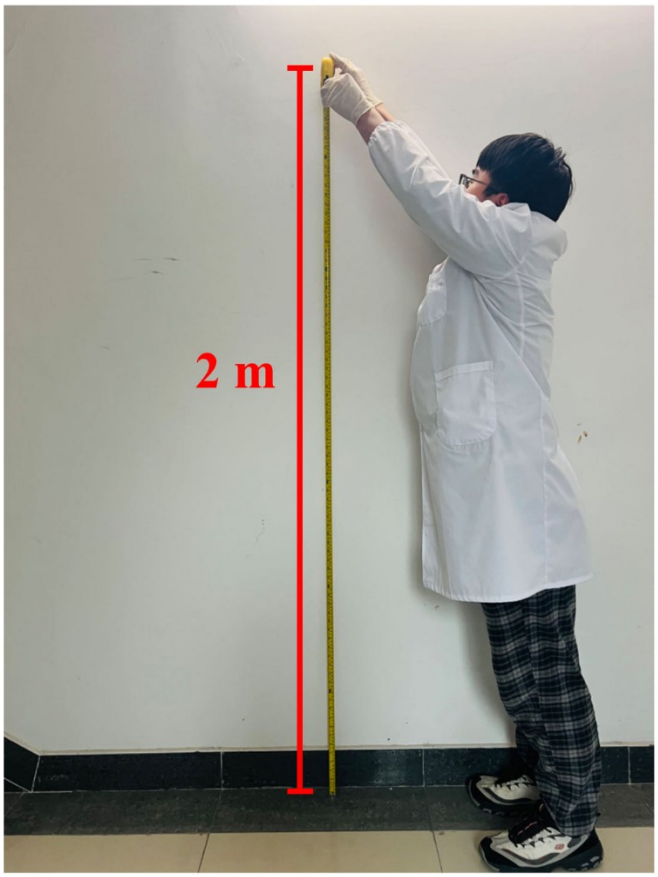

Figure S9. Drop the fully charged battery freely from a height of two meters above the ground and test the open circuit voltage of the battery to detect whether an internal short circuit occurs.

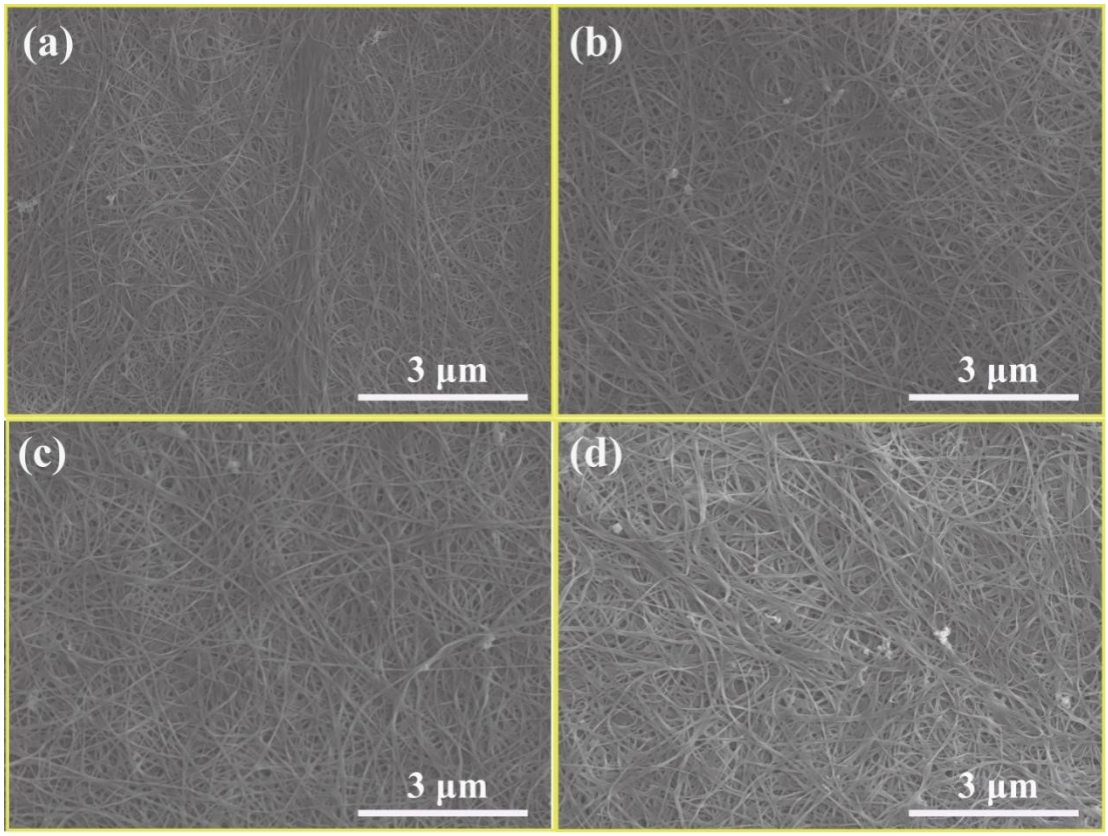

Figure S10. SEM morphology of the front side of different separators (a) BC; (b) PABC-2.5; (c) PABC-5; (d) PABC-7.5.

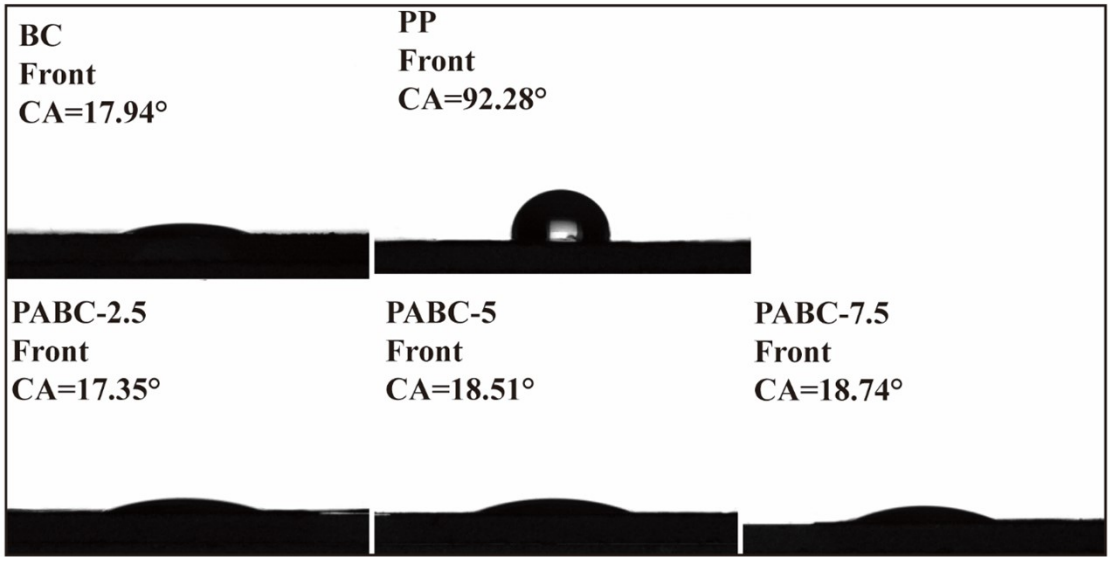

Figure S11. The S surface contact angle of separators' front surface.

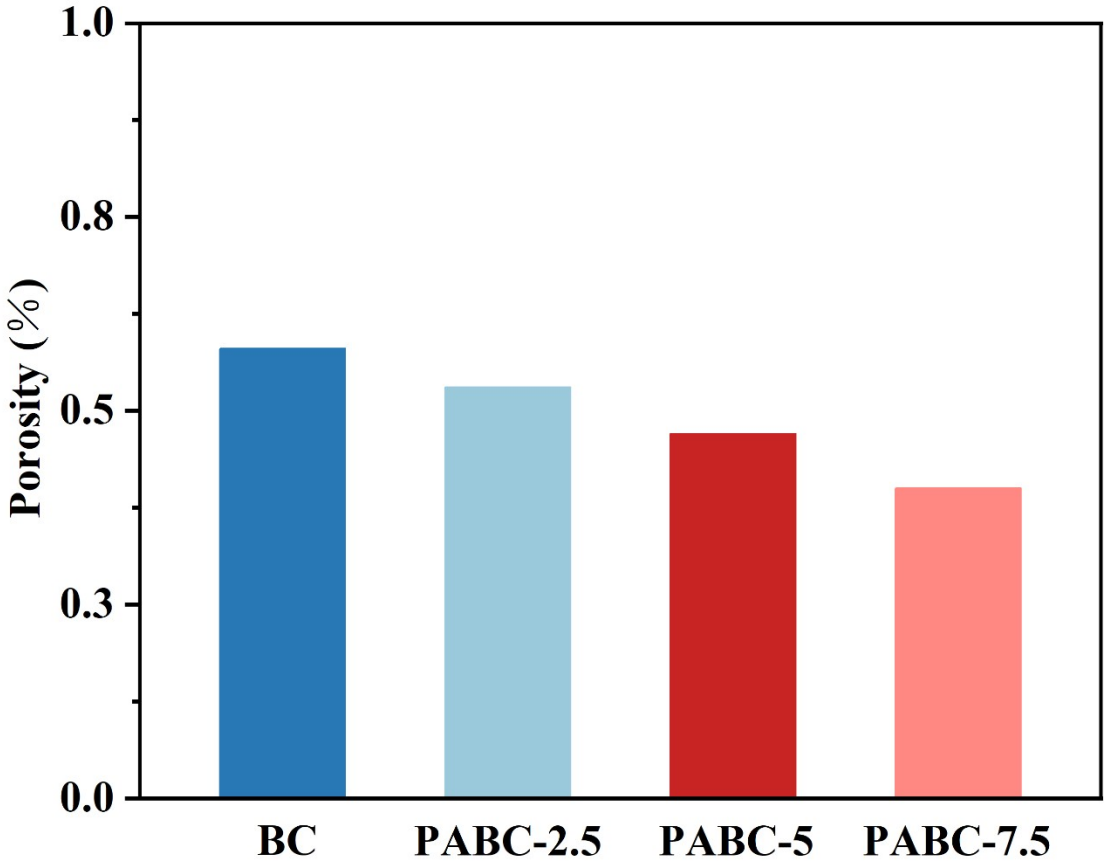

Figure S12. Porosity comparison of separators.

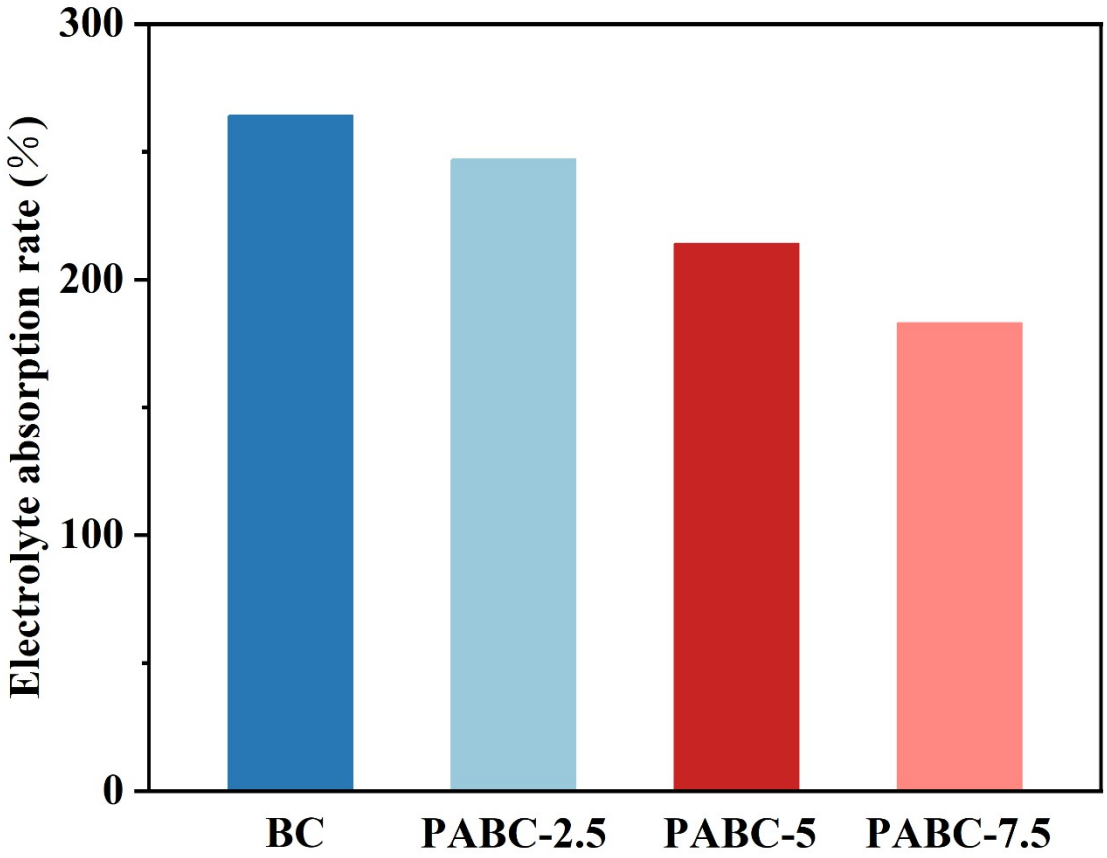

Figure S13. Comparison of electrolyte absorption rate of separators.

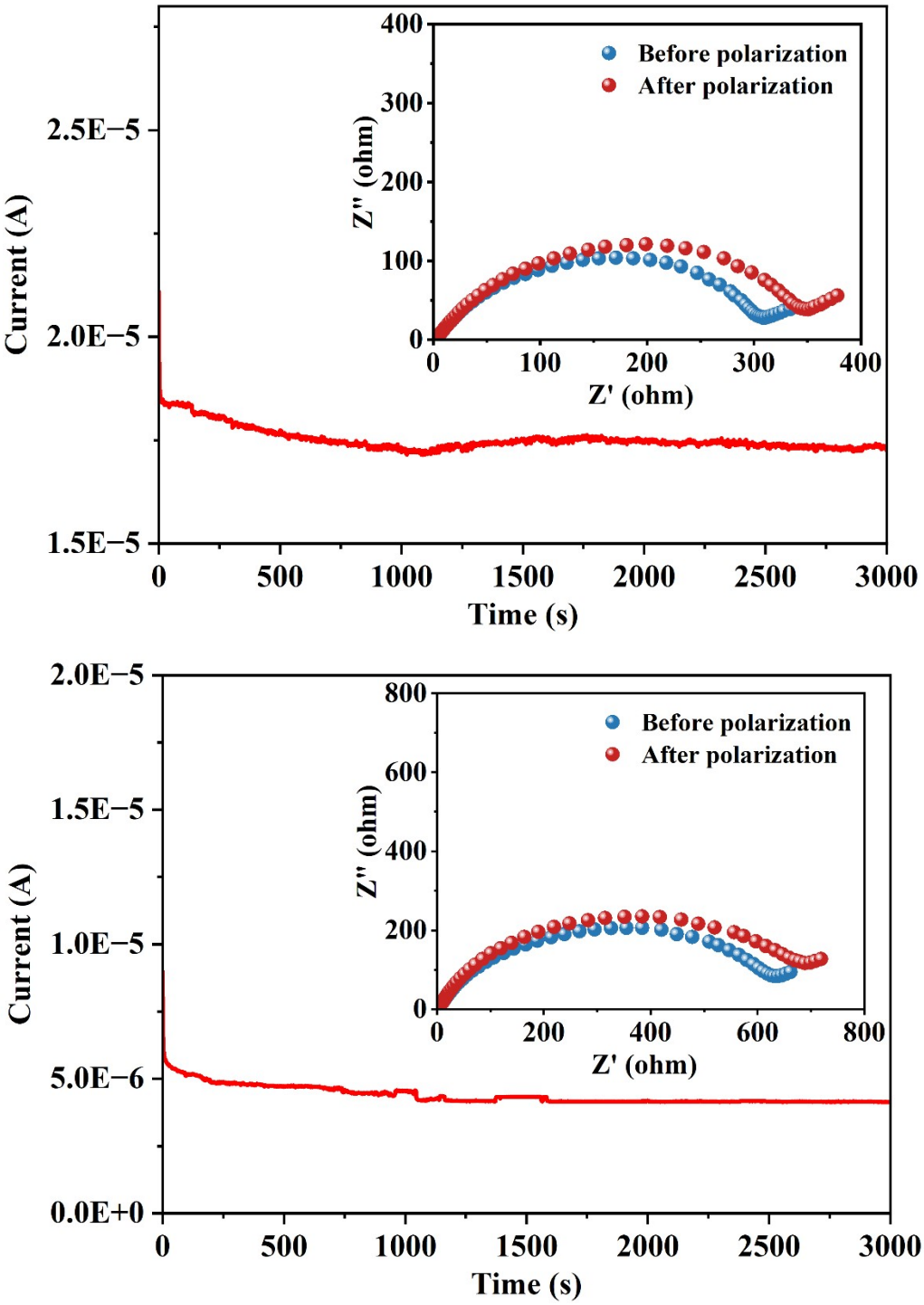

Figure S14. Variation of current with time and EIS tests before and after the polarization of symmetric cells with BC (upper) and PP (lower).

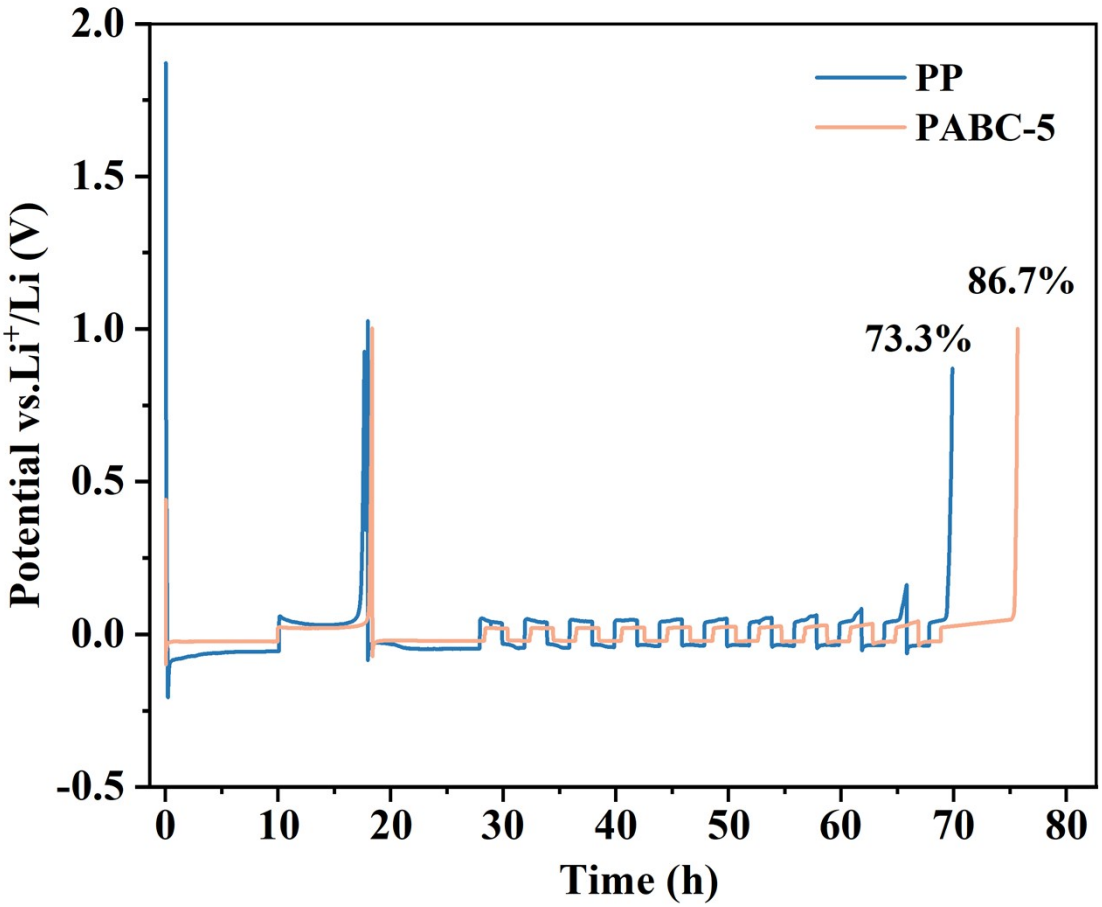

Figure S15. Coulombic efficiency of different separators tested by the Aurbach method via Li||Cu half cells.

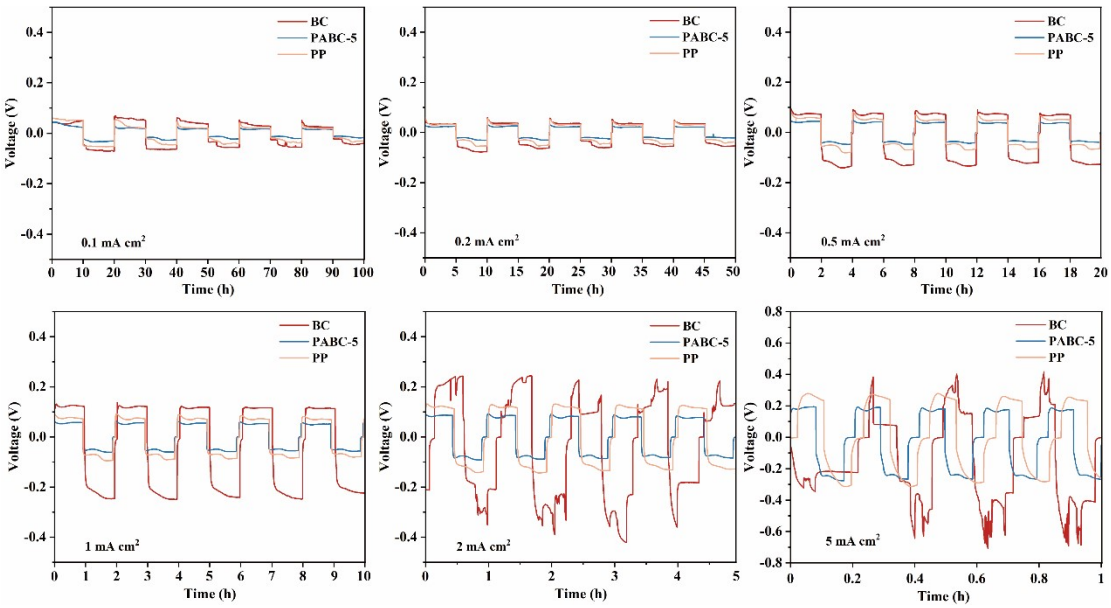

Figure S16. Li stripping and plating stability of the Li//Li symmetric cell with different separators at different current densities from 0.1 to 5 mA cm^{-2}.

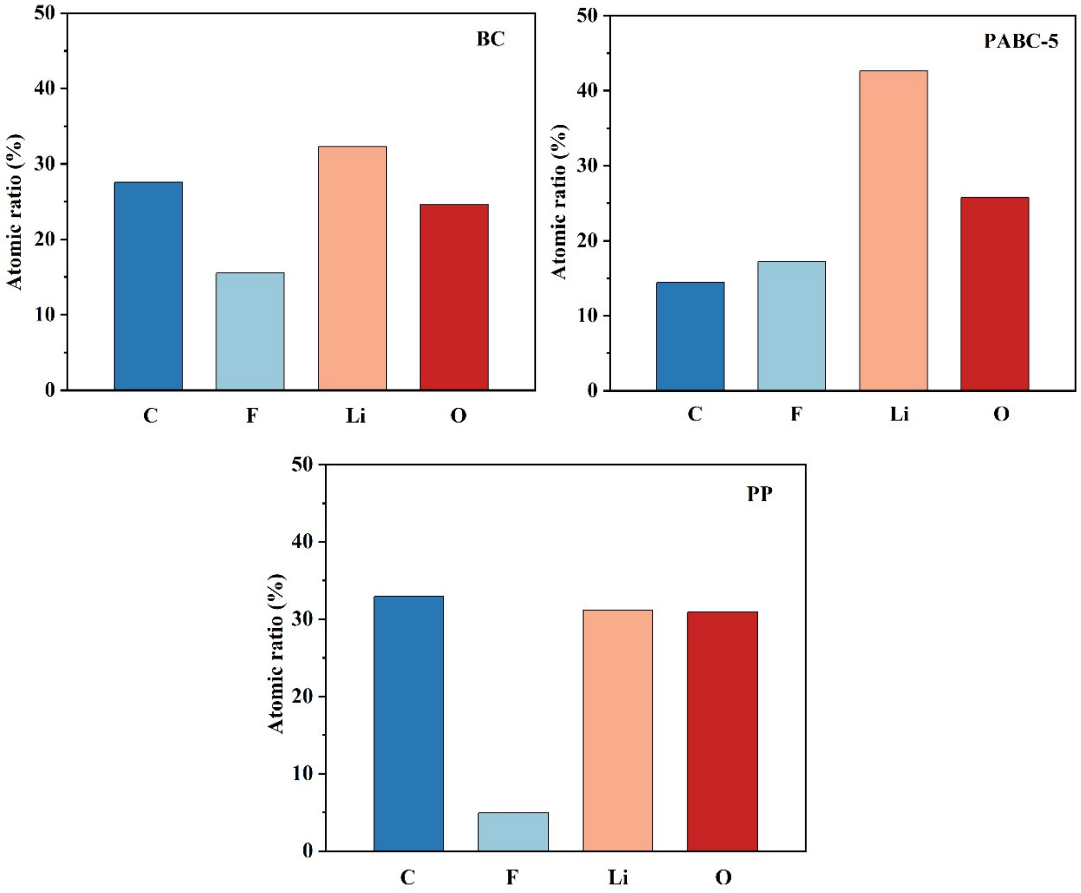

Figure S17. XPS test of the lithium metal surface after cycling of lithium symmetric batteries assembled with different separators, the proportion of each element in the surface SEI layer.

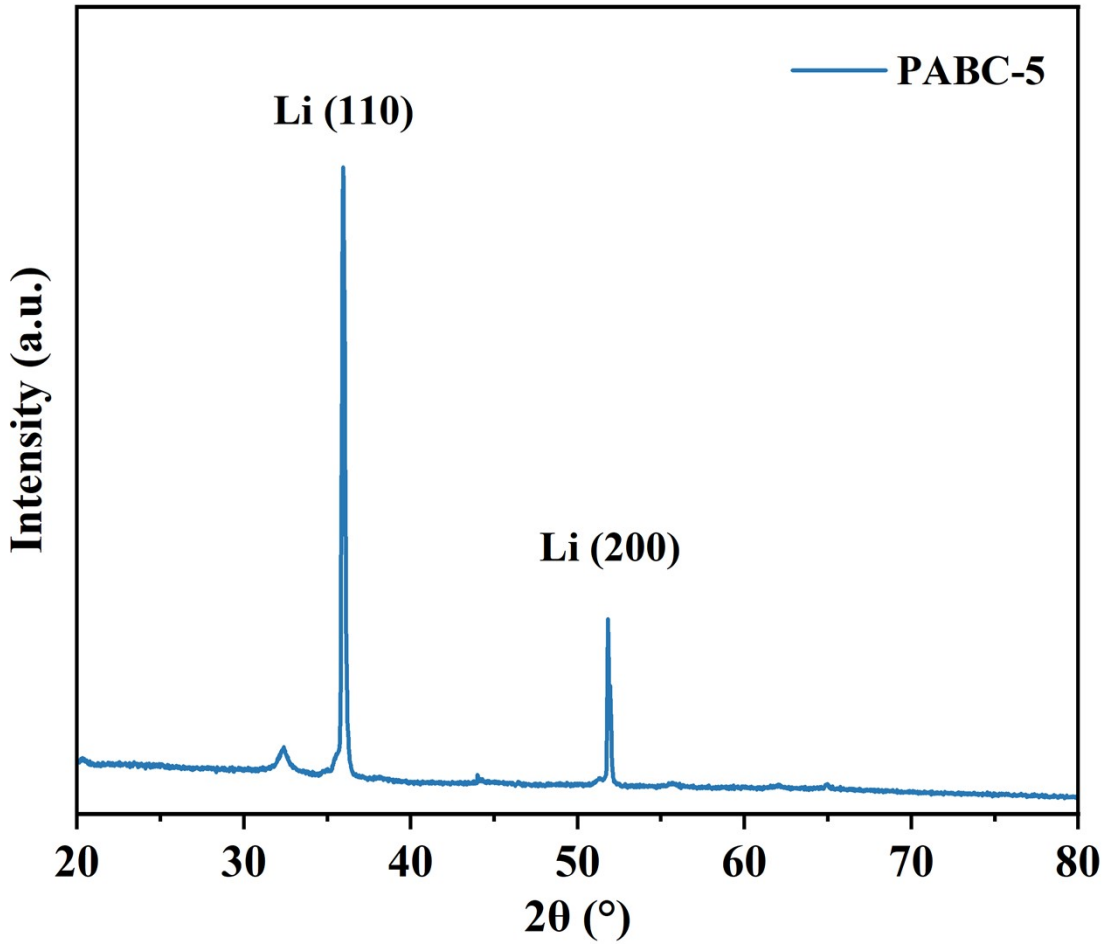

Figure S18. XRD Pattern of Deposited Li in Lithium Symmetric Cells after Cycling.

Table S1. GPC data of PEGDA and AA copolymers.

Peak Molecular Weight (g/mol)	922
Number Average Molecular Weight (g/mol)	653
Weight Average Molecular Weight (g/mol)	1975
Z-Average Molecular Weight (g/mol)	6040
Z+1-Average Molecular Weight (g/mol)	11308
Polydispersity Index (g/mol)	3.02

Table S2. Perform a drop test on the battery charged to 3.8 V and record the number of drops when the battery has an internal short circuit.

	Number of drops before battery short circuit	
Drop test batches	PABC-5	BC
1	74	40
2	78	39
3	63	28
4	67	31
5	61	34
6	72	37
7	76	39
8	71	42
9	73	43
10	75	31

Table S3. Binding energy of PEGDA/AA and BC-chain to Li^+.

	Li^+
PEGDA/AA	0.68 eV
	0.66 eV
	0.65 eV
BC-chain	4.65 eV
	4.43 eV
	3.41 eV
	2.55 eV